A New Alcohol Dehydrogenase with Unique Stereospecificity from *Pseudomonas* sp.

CURT W. BRADSHAW, G.-J. SHEN, AND C.-H. WONG[1]

Scripps Research Institute, Department of Chemistry, 10666 N Torrey Pines Rd., La Jolla, California 92037

A new nicotinamide cofactor-dependent alcohol dehydrogenase from *Pseudomonas* strain SBD6 (PADH) was isolated and purified 150-fold to homogeneity using a combination of salt precipitation, anion-exchange chromatography, gel filtration chromatography, and dye matrix chromatography. Approximately 10 mg of pure enzyme can be obtained from 10 g of wet cells. The enzyme has four subunits with a total molecular weight of 162,000. Incubation with the metal chelators 1,10-phenanthroline, 2-aminoethanethiol, hydroxyquinolinesulfonic acid, N-ethylmaleimide, and potassium cyanide result in complete loss of activity. The enzyme is very stable ($t_{1/2} \sim 7$ days at pH 7 and 25°C in the absence of 2-propanol and ~18 days in the presence of 10% 2-propanol, v/v) and possesses a broad substrate specificity with transfer of the *pro-(R)* hydride from NADH to the *si* face of carbonyl substrates to give (R)-alcohols in high enantiomeric excess, a stereochemical process different from that of other known alcohol dehydrogenases. Synthetic scale reductions are facilitated with 2-propanol as a hydride source for the regeneration of NADH. The kinetic mechanism is ordered bi–bi with the cofactor binding first. Based on NAD and 2-propanol, the kinetic parameters of the enzyme were determined to be $V_{max} = 29.9$ Units mg^{-1} at 25°C and pH 8.5, $K_m^{NAD} = 0.36$ mM and $K_m^{\text{2-propanol}} = 0.19$ mM. © 1991 Academic Press, Inc.

INTRODUCTION

With few exceptions, nicotinamide cofactor (NADH or NADPH)-dependent alcohol dehydrogenase-catalyzed reactions (Fig. 1) follow Prelog's rule, which states that the hydride is transferred from the cofactor to the top face of the carbonyl where the small and large groups are oriented as shown in Fig. 1B to give an (S)-alcohol (*1*). The facial selectivity of alcohol dehydrogenase-catalyzed reduction is usually very high, producing high enantiomeric excess of alcohols.

Several alcohol dehydrogenases have been shown to be useful catalysts for organic synthesis (*2*). As a result of our efforts to expand the utility of these catalysts, we have recently isolated a novel alcohol dehydrogenase with unique stereoselectivity from *Pseudomonas* strain SBD6 which was grown on 1,4-butanediol as sole carbon source. The *Pseudomonas* alcohol dehydrogenase (PADH) catalyzes the transfer of the *pro-(R)* hydride fron NADH to reduce ketones with anti-Prelog stereospecificity, yielding exclusively (R)-alcohols (*3*). We report here detailed studies on the purification and characterization of PADH (*4*).

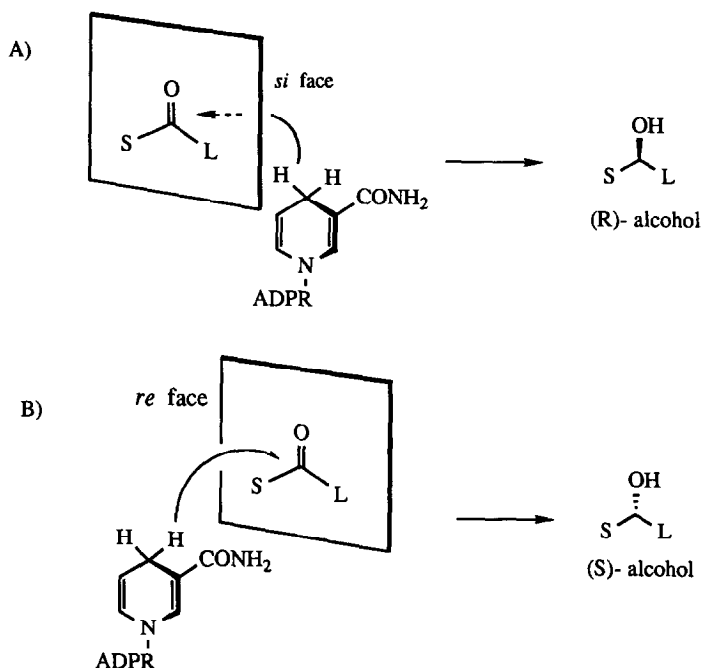[1] To whom correspondence should be addressed.

FIG. 1. (A) Hydride transfer from the nicotinamide cofactor to the *si* face of the carbonyl to give an (*R*)-alcohol. (B) Hydride transfer to the *re* face of the carbonyl to give an (*S*)-alcohol. L, large group; S, small group.

EXPERIMENTAL

Materials and methods. Enzyme activity was routinely measured by incubating 4 mM nicotinamide adenine dinucleotide and 2 mM 2-propanol in 50 mM Tris buffer, pH 8.5, at 25°C. After addition of an aliquot of the enzyme, the change in absorbance was monitored at 340 nm ($\varepsilon = 6220$ mM^{-1} cm^{-1}) with a Beckmann DU-70 spectrophotometer equipped with a temperature controller. One unit of activity is defined as the oxidation of 1 μmol of 2-propanol per minute. Protein concentration was determined by measuring the absorbance at 280 nm (1 mg protein per absorbance unit) or by the bincinchoninic acid assay method (Pierce) with bovine serum albumin as standard. Native and SDS–gel electrophoresis and isoelectric focusing were performed with a Pharmacia Phast system or by the method of Laemmli (5) and the gel was visualized with an established Coomassie staining method (6). DEAE–Sepharose CL-6B was purchased from Pharmacia. Affi-Gel blue affinity chromatography gel was purchased from Bio-Rad. All other chemicals were purchased from Aldrich or Sigma, unless otherwise stated. Nuclear magnetic resonance experiments were performed on a Bruker AM-300 spectrophotometer. All centrifugations were carried out in a Beckmann J2-21 centrifuge. Oxy-Ferm tube kit was purchased from Roche Diagnostic Systems. Amino acid analysis was performed by the protein analysis facility at Scripps.

Microorganism. The organisms were enriched in a screening medium containing (g/liter) NH_4Cl, 1.0; $CaCl_2 \cdot 2H_2O$, 0.05; $MgSO_4 \cdot H_2O$, 0.5; NaCl, 1.0; $NaH_2PO_4 \cdot H_2O$, 2.1, K_2HPO_4, 0.3; yeast extract, 0.2; and trace mineral solution, 10 ml. The trace mineral solution contained (g/liter) nitriloacetic acid, 12.8; $FeSO_4 \cdot H_2O$, 0.1; $MnCl_2 \cdot 4H_2O$, 0.1; $CoCl_2 \cdot 6H_2O$, 0.2; $CaCl_2 \cdot H_2O$, 0.1; $ZnCl_2 \cdot 2H_2O$, 0.1; $CuCl_2 \cdot 2H_2O$, 0.02; H_3BO_3, 0.01; $Na_2MoO_4 \cdot 2H_2O$, 0.01; NaCl, 1.0; Na_2SeO_3, 0.02; $NiSO_4 \cdot 6H_2O$, 0.03; and Na_2WO_4, 0.02. The pH of the medium was adjusted to 7.0. 1,4-Butanediol was added as a carbon and energy source (0.5%, v/v). The enrichment was carried out at 30°C with shaking (250 rpm) in serum bottles (125 ml) containing 20 ml of medium and 0.1 g of garden soil as the source of microorganisms. The enrichments which showed growth were then plated onto agar plates prepared from the screening medium containing 1.5% agar. Subsequently, single colonies were transferred into serum bottles containing 20 ml of the same medium. These procedures were repeated several times and finally, the cultures were plated on LB agar plates (tryptone, 10 g; yeast extract, 5 g; NaCl, 0.5 g; 15 g agar per liter distilled water, pH 7.0) to ensure homogeneity of the colonies. The cell morphology was observed under a microscope. Physiological characterization was carried out with an Oxy-Ferm tube kit. The characteristics of the genus were determined according to established procedures (7).

Enzyme purification. All purification steps were done at 4°C unless stated otherwise. A single colony was transferred to a serum bottle containing 20 ml of the screening medium. The growing culture was then transferred to a 3-liter flask containing 1 liter of the same medium with 0.5% 1,4-butanediol as carbon source. The culture was cultivated aerobically at 30°C with shaking (250 rpm) and monitored by measuring the optical density at 660 nm. In a typical procedure, cell cultures (3 liter total volume) obtained during the late exponential growth phase (OD ~ 1.5–2.0) were harvested by centrifugation at 8000 rpm for 15 min. The wet cells (10 g) were suspended in 5 mM dithiothreitol (1 g wet cells/5 ml DTT solution) and ruptured in a SLM Aminco French press (23,000 psi). Cell extract was obtained as the supernatant after centrifugation at 15000 rpm for 90 min. The ammonium sulfate pellet obtained from precipitation at 40–70% saturation was dialyzed for 6 h versus 30 mM Tris buffer, pH 8, containing 1.25 mM DTT and 0.25 mM zinc sulfate (buffer A). The enzyme solution was loaded on a DEAE–Sepharose CL-6B column (2.5 × 45 cm) previously equilibrated with buffer A. The column was washed with buffer A until the nonbinding components which absorb at 280 nm were eluted. Subsequently, a linear 100–300 mM ammonium acetate gradient in buffer A (1000 ml) was carried out. The fractions containing NAD-dependent alcohol dehydrogenase activity were concentrated in an Amicon protein concentrator (PM 10 filter) and applied to a G-200 Sephadex gel filtration column (2.5 × 95 cm) and eluted with buffer A at a flow rate of 6 ml/h. The desired enzyme fractions were concentrated as before in an Amicon protein concentrator. Following dialysis in 30 mM Tris buffer, pH 7, containing 1.25 mM DTT and 0.25 mM zinc sulfate (buffer B) for several hours, the solution was applied to an Affi-Gel blue affinity column (1 × 15 cm) equilibrated with buffer B. After washing with buffer B until no more protein eluted, as determined by absorbance at 280 nm, the alcohol dehydrogenase was eluted with 5 mM NAD in buffer A, flow rate 1.5 ml/h.

Determination of the stereospecificity of hydride transfer. The procedure followed was the same for each enzyme. The enzyme [11 units horse liver alcohol dehydrogenase, 20 units PADH, 30 units yeast alcohol dehydrogenase, 12 units *Thermoanaerobium brockii* alcohol dehydrogenase, or 50 units glucose dehydrogenase (*Bacillus* sp., Amano)] was dissolved in 2 ml of the reaction solution, containing 5 mM bicarbonate buffer, pH 8, 4 mM nicotinamide adenine dinucleotide (NAD, NADP for *T. brockii*), a deuterated substrate [either 180 mM 2-propanol-d_8 (for PADH, *T. brockii,* yeast alcohol dehydrogenase), 180 mM ethanol-d_6 (for horse liver alcohol dehydrogenase), or 55 mM deuterated glucose (for glucose dehydrogenase)], and 1 mg of sodium azide, and placed in a previously washed dialysis tube (SpectraPor2 MWCO 12–14,000). The dialysis tube was inserted into 10 ml of the reaction solution and was stirred for 3 days. The tube was then removed and rinsed with distilled water. The washings and reaction solution were combined and lyophilized. The resulting powders were dissolved in 10 mM ammonium bicarbonate buffer, pH 8, and applied to a DEAE–cellulose column (1.5 × 8 cm). Excess unreacted NAD was eluted with 50 mM ammonium bicarbonate buffer, pH 8. The monodeuterated NADH was subsequently eluted with 250 mM ammonium bicarbonate buffer. The fractions absorbing at 340 nm were collected and lyophilized several times, twice versus deuterium oxide to remove water. The precipitate was dissolved in deuterium oxide containing sodium 3-(trimethylsilyl)-1-propanesulfonate as an internal standard for NMR measurement.

Kinetic determinations. For initial velocity and product inhibition studies, acetone was distilled over potassium permanganate and stored over 4-Å sieves. 2-Propanol was distilled over magnesium and iodine, run through an alumina column, and stored over 4-Å sieves. Aliquots of the appropriate stock solutions (all in the assay buffer, 50 mM Tris, pH 8.5) containing 20 mM 2-propanol, 20 mM acetone, 40 mM NAD, 10 mM NADH, and the assay buffer were equilibrated at 25°C. Reactions were begun by addition of enzyme and monitored at 340 nm. The initial velocities were recorded and analyzed according to the methods of Cleland to determine initial velocity and product inhibition patterns (*8*). K_m and k_{cat} values were determined according to established methods. The slopes and intercepts of the Lineweaver–Burk plots of inverse rate versus inverse 2-propanol concentrations at different constant concentrations of NAD were replotted to determine K_m and V_{max}.

Inactivation with metal chelators. The enzymatic activity was measured at various intervals under standard assay conditions (see general methods) after incubation in the presence of 16 mM EDTA, 20 mM picolinic acid, 11 mM 2,2-dipyridyl, 50 mM sodium azide, 35 mM thiourea, 14 mM 4,7-phenanthroline, 45 mM *N*-ethylmaleimide, 12 mM hydroxyquinoline sulfonic acid, 14 mM 1,10-phenanthroline, 30 mM potassium cyanide, or 0.75–30 mM 2-aminoethanethiol. The second-order rate constant was calculated using

$$\ln(E_t/E_0) = -k''Yt$$

where E_0 is the initial enzyme activity, E_t is the enzyme activity at time, t, Y is the concentration of the added compound, and k'' is the second order rate constant.
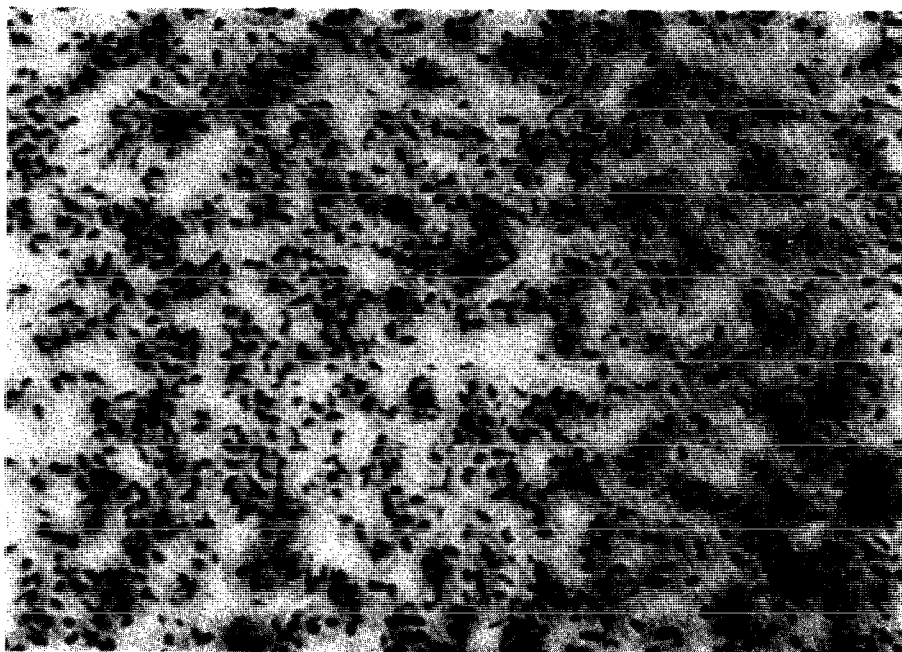
FIG. 2. *Pseudomonas* strain SBD6.

2-Aminoethanethiol-inactivated PADH (1 ml) was dialyzed overnight against 25 mM Tris buffer containing 0.5 mM zinc sulfate (500 ml) in an attempt to regain enzyme activity. Protection against inactivation was shown with 2-aminoethanethiol using the same procedure but at low concentrations (150 μM) and saturating concentrations (2 mM) of 2-propanol.

Isoelectric focusing. The isoelectric point of purified PADH was compared to

TABLE 1

Physiological Characteristics of
Pseudomonas Strain SBD6

Characteristic	Result
OF anaerobic dextrose	Negative
Arginine dihydrolase	Positive
H$_2$S formation	Negative
Indole formation	Negative
OF xylose	Positive
OF aerobic dextrose	Positive
Urease	Positive
Citrate utilization	Positive
Oxidase	Positive

TABLE 2

Purification of *Pseudomonas* Alcohol Dehydrogenase from 10 g of Wet Cells

Step	Volume (ml)	Activity (Units)	Protein (mg)	Specific activity (U/mg)	−Fold	Yield (%)
French press	86	1033	5084	0.2	1	100
Ammonium sulfate precipitation	52	992	2146	0.46	2.3	96
DEAE-Sepharose CL-6B	14	806	512	1.57	7.9	78
Sephadex G-200	8	444	194	2.29	11.4	43
Affi-Gel blue	3	299	10	29.9	150	29

standards (Sigma) using the Pharmacia Phast system. After initial determination with IEF 3–10 gel, an accurate value was obtained with the IEF 4–6.5 gel. The methods were followed according to the manufacturer and the gels are available from Pharmacia.

pH profile. Solutions containing 2.5 mM NAD, 2 mM 2-propanol, 100 mM Mops and 100 mM L-histidine (final concentrations, V_{max} conditions) at pH values from 6 to 10 were equilibrated at 25°C. The change in absorbance was monitored at 340 nm after addition of enzyme. Alternatively, solutions from pH 6 to 10 containing 0.4 mM NADH, 2 mM acetone, 100 mM Mops, and 100 mM L-histidine were treated in the same manner. Initial velocities were recorded for comparison.

Temperature dependence of enzyme activity and stability. In order to examine temperature dependence on enzyme activity, the assay solution composed of 3
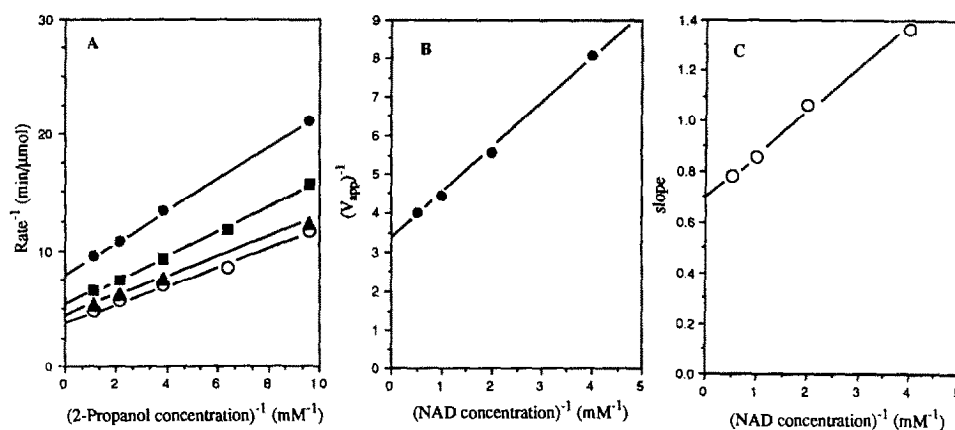
FIG. 3. Determination of kinetic constants: (A) Lineweaver–Burke plot for rate versus 2-propanol, ● 0.25 mM NAD, ■ 0.5 mM NAD, ▲ 1 mM NAD, ○ 2 mM NAD; the y intercepts are values of $1/V_{app}$ at different concentrations of NAD. (B) Replot of $1/V_{app}$ versus 1/NAD where the y intercept is $1/V_{max}$ and the x intercept is $-1/K_m$ for NAD. (C) Replot of slopes versus 1/NAD, the y intercept is K_m/V_{max} for 2-propanol. See Experimental for details.
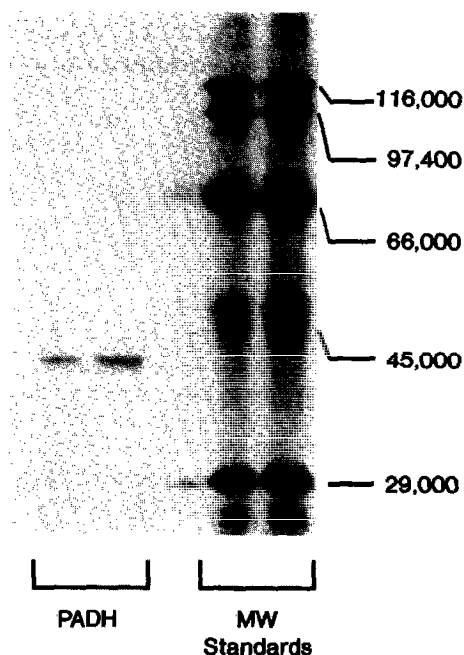
FIG. 4. SDS–PAGE of PADH. The molecular weight markers used include carbonic anhydrase (29,000), egg albumin (45,000), bovine albumin (66,000), phosphorylase B (97,400), and β-galactosidase (116,000).

mM NAD and 2 mM 2-propanol in 50 mM Hepes buffer, pH 8, was equilibrated at temperatures from 30 to 70°C $\pm$ 0.5°C in a water bath. Reaction was begun by addition of enzyme and monitored as previously stated. The spectrophotometer was equipped to maintain constant temperature. To determine temperature stability, pure PADH in 50 mM Hepes buffer, pH 8, was incubated at temperatures from 30 to 75°C. To determine the stability at room temperature, the enzyme was dissolved in a 50 mM phosphate buffer, pH 7. At appropriate intervals, an aliquot was removed and assayed at 25°C as described above. The half-life was determined according to equations,

$$\ln C/C_0 = -kt,$$

where C_0 is the initial enzyme activity, C is the activity at time, t, and k is the rate constant. The half-life $(t_{1/2})$ is defined to be

$$t_{1/2} = \ln 2/k.$$

The initial velocity data at various temperatures was used to calculate the activation parameters $\Delta H\ddagger$, enthalpy of activation, and $\Delta S\ddagger$, entropy of activation based on the Eyring equation:

$$k = (KT/h)e^{-\Delta H\ddagger/RT_e\Delta S\ddagger/R},$$
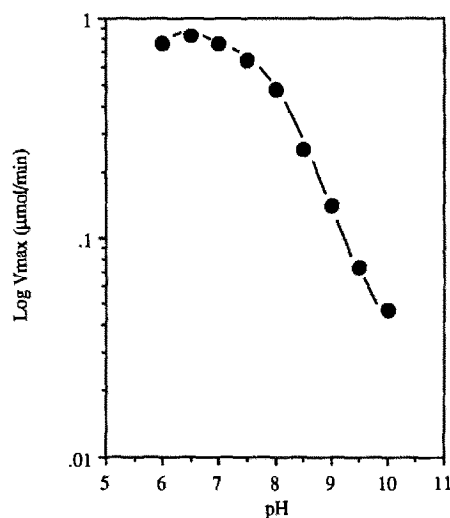
FIG. 5. pH Profile for the reduction of acetone. See Experimental for details.

where K is the Boltzmann constant $(1.381 \times 10^{-23} \text{ J/K})$, h is the Planck constant $(6.6262 \times 10^{-34} \text{ J/s})$, R is the gas law constant $(8.314 \text{ J/mol K or } 1.987 \text{ cal/mol K})$, T is the temperature in kelvin and k is the rate constant (k_{cat}). A plot of k versus T can be fitted to the equation using a nonlinear least-squares regression program (Enzfitter from Biosoft) to obtain the values directly. Alternately, the equation may be rearranged to give
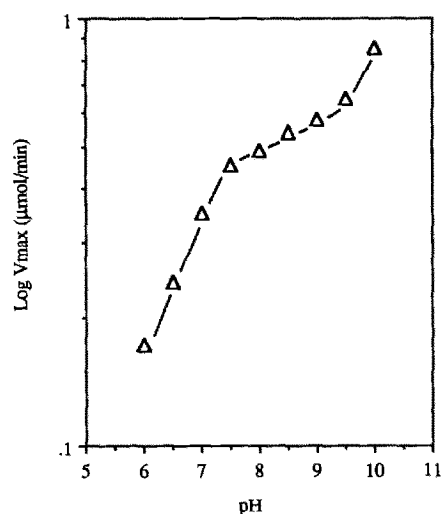
FIG. 6. pH Profile for the oxidation of 2-propanol. See Experimental for details.
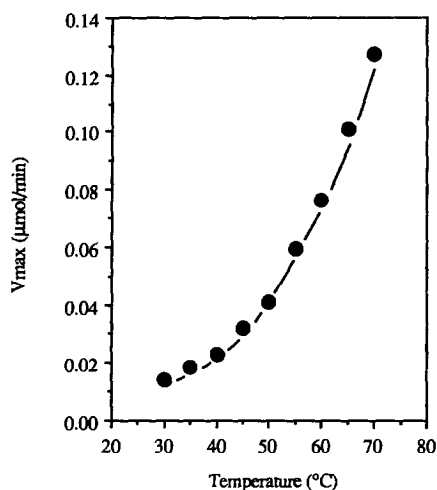
Fig. 7. Temperature optimum for PADH. See Experimental for details.

$$\ln k/T = -\ln K/h - \Delta H\ddagger/RT + \Delta S/R.$$

A plot of ln k/T versus $1/T$ will give $-\Delta H\ddagger/R$ as the slope and $(\Delta S/R - \ln K/h)$ as the y intercept, from which the parameters can be calculated using the constant values.

Molecular weight determination. Purified PADH was injected onto a Pharmacia Superose 12 column using buffer A at a flow rate of 0.3 ml/min. The absorbance of the eluent was monitored continuously at 280 nm and the tubes were assayed to ensure identification of active enzyme. The retention time of PADH was compared to the retention times of molecular weight standards (Sigma), with migration proportional to the log of the molecular weight. Retention times were determined as the mean of at least three injections. SDS-denatured enzyme was compared
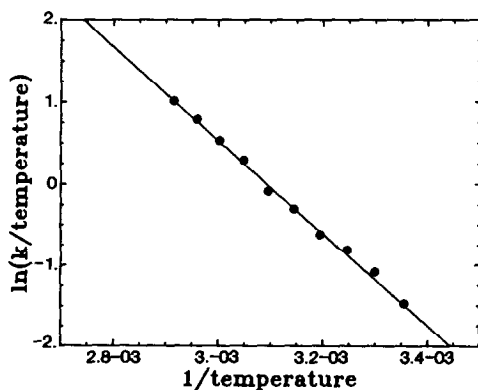
Fig. 8. Eyring plot for the PADH-catalyzed oxidation of 2-propanol.

TABLE 3

Amino Acid Composition of
Pseudomonas Alcohol
Dehydrogenase

Residue	Number/enzyme[a]
Ala	187.6 ± 4.5
Asp	114 ± 1.2
Arg	34.6 ± 0.5
Gly	330.8 ± 7.8
Glu	115.4 ± 1.9
His	33.6 ± 3.2
Ile	90.0 ± 1.7
Leu	105.8 ± 2.9
Lys	69.5 ± 2.1
Met	31.9 ± 0.8
Phe	26.0 ± 1.5
Pro	62.6 ± 1.5
Ser	57.7 ± 0.7
Thr	76.3 ± 5.2
Tyr	19.0 ± 2.7
Val	141.8 ± 1.4

[a] Represents the number of residues per molecule of tetrameric enzyme. Residue amounts were calculated by normalizing peak areas of three composition determinations with 112 μg of pure PADH.

versus electrophoresis standards (Sigma), using electrophoretic methods as detailed under Materials and Methods and Isoelectric Focusing with the Pharmacia system.

Substrate specificity. The specificity of PADH was determined in both oxidative and reductive directions by monitoring the presence of NADH at 340 nm. The relative rates of oxidation were determined in 50 mM Tris buffer, pH 8.5, containing 4 mM NAD and 10 mM of various alcohols at 25°C. The relative rates were taken as the initial velocity with 2-propanol arbitrarily set to be 100. With respect to ketones, the relative rates were measured in 0.15 M Tris buffer, pH 7.1, with 0.45 mM NADH and 3 mM the ketone. The relative rate was arbitrarily set at 100 with 2-propanone. For large scale synthesis, enzyme was prepared as described previously (*3*). Phosphate buffer (10 mM, pH 7.0) containing NAD (20 mg), 2-propanol (12.2 ml), 20 mmol of various ketones, and enzyme with a total volume of 75 ml was stirred at room temperature. The rate of substrate consumption was monitored by gas chromatography. When all the substrate was consumed, the mixture was extracted with dichloromethane (3 × 100 ml) and the combined organic phase dried over sodium sulfate. After solvent evaporation, the product
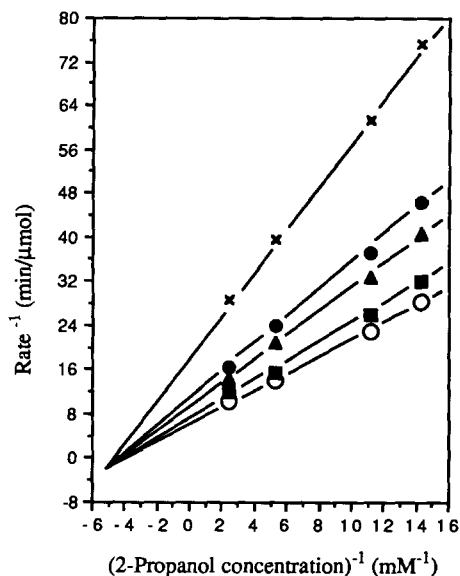
FIG. 9. Reciprocal plot of rate versus 2-propanol concentation at different concentrations of acetone: ○ 0 mM acetone, ■ 0.14 mM acetone, ▲ 0.28 mM acetone, ● 0.42 mM acetone, × 1.0 mM acetone. The concentration of NAD was fixed at 0.9 mM. See Experimental for details.

was purified via silica gel chromatography to determine yield. Enantiomeric excess was measured by comparison of optical rotation versus known compounds or by conversion to a Mosher ester and determined with ^{1}H NMR at 300 MHz (3).

RESULTS AND DISCUSSION

Microorganism identification. The microorganism is a gram negative motile obligate aerobe and is a short rod with a diameter of 0.5–1 μm (Fig. 2). Colonies are cream color with a round edge. Young colonies have a smooth surface, but become rough with age. The physiological characteristics are summarized in Table 1. Thus, the organism was identified as belonging to the *Pseudomonas* species and assigned as *Pseudomonas* strain SBD6.

Purification. A representative enzyme purification is shown in Table 2. The individual procedures were followed as described previously (9). Following ammonium sulfate precipitation, the desired enzyme fraction could be dialyzed for as little as 2 h without adversely affecting the binding to the anion-exchange column. After eluting the alcohol dehydrogenase from the DEAE–Sepharose CL-6B column with a salt gradient, the gel filtration column served to desalt and further purify the enzyme. Although the yield from the gel filtration column was relatively low, the step proved essential in obtaining pure enzyme after the dye matrix chromatography. Binding of the enzyme to Affi-Gel blue was optimal at pH 7.
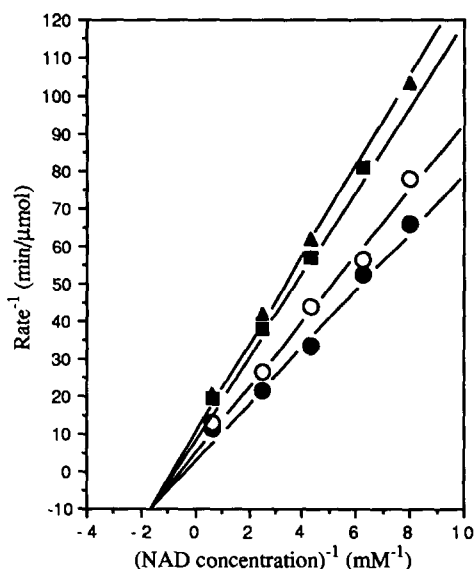
Fig. 10. Reciprocal plot of rate versus NAD concentration at different concentrations of acetone: ● 0 μM acetone, ○ 200 μM acetone, ■ 400 μM acetone, ▲ 600 μM acetone. The concentration of 2-propanol was fixed at 0.3 mM. See Experimental for details.

Raising the pH to 8, where the enzyme is most stable, after binding to the dye matrix did not elute the enzyme. Elution from the affinity matrix could only be affected by addition of NAD to the buffer. The enzyme was judged to be pure by several criteria; single bands with SDS–PAGE, native electrophoresis, and isoelectric focusing. Additionally, one peak containing all enzyme activity was observed with high resolution gel filtration (Pharmacia FPLC, Superose 12). From 10 g of wet *Pseudomonas* cells, 10 mg of homogeneous enzyme was obtained with an overall yield of 29% after a 150-fold purification. Kinetic parameters were determined based on NAD and 2-propanol; V_{max} = 29 U mg^{-1} at 25°C, pH 8.5, K_m^{NAD} = 0.36 mM, and $K_m^{2\text{-propanol}}$ = 0.19 mM (Fig. 3). The same methods yielded the Michaelis constants K_m^{NADH} = 0.17 and $K_m^{acetone}$ = 0.31 mM for acetone and NADH.

Characterization. The molecular weight of the denatured alcohol dehydrogenase determined by SDS–PAGE is 41,000 (Fig. 4). The molecular weight of the native enzyme determined by high resolution gel filtration (Superose 12 FPLC) is 162,000, indicating the enzyme exists as a tetramer in solution. Pure enzyme had a single protein peak from the gel filtration with which all activity was associated. The isoelectric point of the enzyme is 4.7 ± 0.1.

The pH optimum of PADH for reduction of acetone was 6.5 (Fig. 5), while in the oxidation of 2-propanol, the rate did not decrease at pH values up to 10.0 (Fig. 6). The activity of PADH for oxidation of 2-propanol at pH 8.5 continually increased with increasing temperature up to 70°C (Fig. 7). The K_m values for NAD and 2-propanol remained relatively constant (K_m 2-propanol was 190 μM at 25°C

BRADSHAW, SHEN, AND WONG
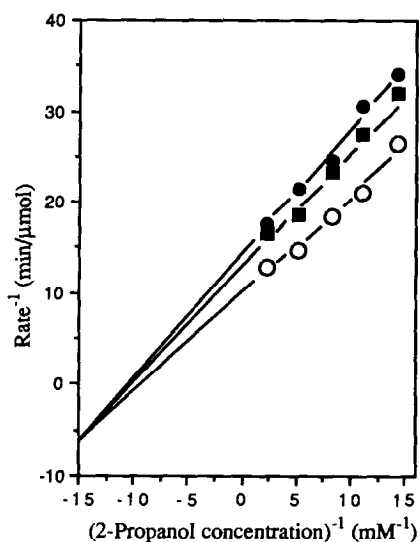
FIG. 11. Reciprocal plot of rate versus 2-propanol concentration at different concentrations of NADH: O 0 mM NADH, ■ 0.15 mM NADH, ● 0.35 mM NADH. The concentration of NAD was fixed at 0.6 mM. See Experimental for details.
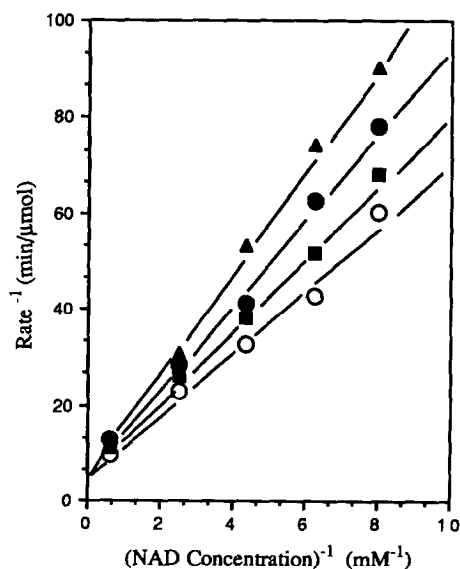
FIG. 12. Reciprocal plot of rate versus NAD concentration at different concentrations of NADH: ■ 0 μM NADH, ■ 75 μM NADH, ● 150 μM NADH, ▲ 350 μM NADH. The concentration of 2-propanol was fixed at 0.3 mM. See Experimental for details.
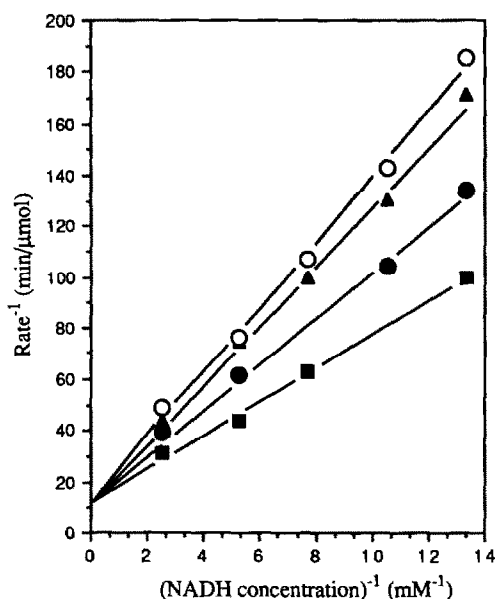
FIG. 13. Reciprocal plot of rate versus NADH concentration at different concentrations of NAD: ■ 0 μM NAD, ● 175 μM NAD, ▲ 350 μM NAD, ○ 550 μM NAD. The concentration of acetone was fixed at 0.6 mM. See Experimental for details.

and 210 μM at 50°C) so that the enzyme was saturated at all temperatures. PADH does not have extraordinary thermostability with half-lives at 35, 45, 55, 65 and 75°C of 412, 119, 13.5, 3.1, and 0.31 min, respectively, as determined in 50 mM Hepes buffer, pH 8. However, the enzyme is very stable at room temperature. The half-life at pH 7 in phosphate buffer is about 7 days whereas in the presence of added 2-propanol (10% v/v) the half-life is about 18 days.

The activation parameters for the oxidation of 2-propanol were determined using the Eyring equation. The data are shown in Fig. 8. The enthalpy of activation ($\Delta H\ddagger$) is 11.3 kcal/mol and the entropy of activation ($\Delta S\ddagger$) is -12.2 e.u. The low enthalpy of activation suggests the reaction will proceed readily at room temperature.

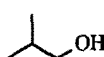Incubation of purified enzyme with various metal chelators revealed a time-dependent inactivation of the enzyme. However, several metal chelators including
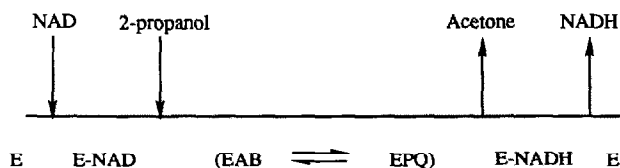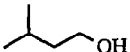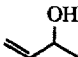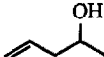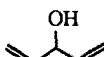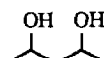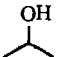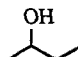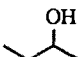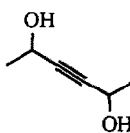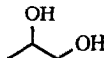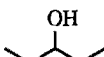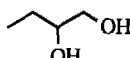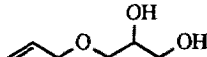
FIG. 14. Kinetic mechanism of PADH.
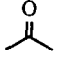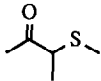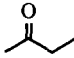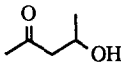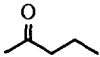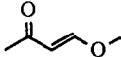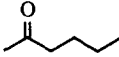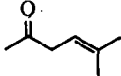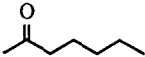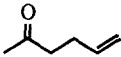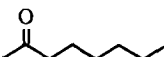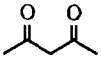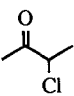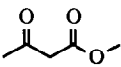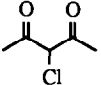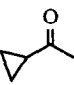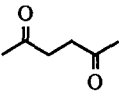
TABLE 4A

PADH-Catalyzed Oxidation of Alcohols

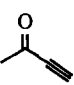| Compound	Relative rate[a]	Compound	Relative rate[a]
CH₃CH₂—OH	0.9	(CH₃)₃C—CH₂—OH	0.04
CH₃CH₂CH₂—OH	2.1	CH₂=C(CH₃)—CH(OH)—CH₃	92
CH₃CH₂CH₂CH₂—OH	0.16	CH₂=CH—CH₂—CH(OH)—CH₃	10
CH₃(CH₂)₄—OH	0.03	CH₂=C(CH₃)—CH(OH)—CH=CH₂	58
CH₃(CH₂)₅—OH	0.03	CH₃—CH(OH)—CH₂—CH(OH)—CH₃	<0.01
(CH₃)₂CH—OH	100	(CH₃)₂C(OH)—CH(OH)—CH₃	0.75
CH₃—CH(OH)—CH₂CH₃	55	(CH₃)₂C(OH)—C≡C—CH(OH)—CH₃	0.04
CH₃CH₂CH₂—CH(OH)—CH₃	4.5	(CH₃)₂C(OH)—CH₂—OH	6.3
CH₃CH₂—CH(OH)—CH₂CH₃	2.8	CH₃CH₂—CH(OH)—CH(OH)—CH₃	0.12
H₂N—CH₂CH₂CH₂—OH	0	CH₂=CH—CH₂—O—CH₂—CH(OH)—CH₂—OH	<0.01
HO—CH₂CH₂CH₂—OH	<0.01		
HO—CH₂CH₂CH₂CH₂—OH	0.17		
HO—(CH₂)₅—OH	0.06		
HO—CH₂—CH=CH—CH₂—OH	0.27		
(CH₃)₂CH—CH₂—OH	0.24		

[a] The rate was determined by monitoring the change in absorbance at 340 nm in 50 mM Tris buffer, pH 8.5. The concentration of NAD was 4 mM and the concentration of all compounds was 6 mM.

EDTA, picolinic acid, 2,2-dipyridyl, sodium azide, and thiourea did not affect the enzyme. The kinetics for inactivation was found to be first order with respect to the chelator concentration. The second-order rate constants for inactivation at pH 8 were as follows: 2-aminoethanethiol, 22 M^{-1} min^{-1}; potassium cyanide, 7.5 M^{-1} min^{-1}; 1,10-phenanthroline, 0.42 M^{-1} min^{-1}; hydroxyquinolinesulfonic acid, 0.28

TABLE 4B

PADH-Catalyzed Reduction of Ketones

Compound	Relative rate[a]	Compound	Relative rate[a]
ketone (acetone)	100	thioester ketone	0
methyl ethyl ketone	42	hydroxy ketone	0
2-pentanone	1.0	enol ether ketone	0
2-hexanone	0.2	unsaturated methyl ketone	0.2
2-heptanone	0.04	allyl ketone	2.6
2-octanone	0.03	2,4-diketone	0.1
chloro ketone	2.7	keto ester	0.1
butynone	58	chloro diketone	132
cyclopropyl ketone	0.5	keto aldehyde ester	0
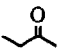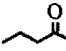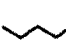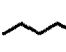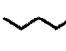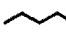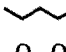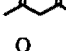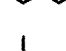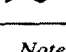
[a] The rate was determined in 0.15 M TRIS buffer, pH 7.1, at 0.45 mM NADH and 3 mM of all substrates.

M^{-1} min^{-1}; and *N*-ethylmaleimide, 0.06 M^{-1} min^{-1}. An isomer of the inactivator 1,10-phenanthroline, 4,7-phenanthroline, which is incapable of efficient metal binding, did not cause any observable inactivation over the course of several hours. Enzymatic activity of 2-aminoethanethiol-inactivated PADH was partially restored to 50% of original activity after overnight dialysis against a buffer containing 0.25 mM zinc sulfate. Further studies are underway to determine the stoichiometry and identity of metal in PADH.

Amino acid composition. The amino acid composition determined for a homogenous preparation of tetrameric alcohol dehydrogenase is shown in Table 3.

Kinetic mechanism. The initial velocity patterns for the oxidation of 2-propanol by NAD and the reduction of acetone by NADH are intersecting, supporting a sequential mechanism. Further evidence for a sequential mechanism was obtained via product inhibition studies. In the oxidation of 2-propanol, acetone is a noncom-

TABLE 4C

Substrate Specificity of PADH for the Reduction of Ketones

Substrate	Relative rate[a]	% ee[b]	% yield	$[\alpha]_D^{25}$ c = 1 ~ 2, $CHCl_3$
(structure)	2.2	87	62	−9.41
(structure)	1.5	97	60	−12.8
(structure)	1.0	>98	70	−10.5
(structure)	0.8	>98	75	−13.2
(structure)	0.5	>98	62	−8.8
(structure)	0.1	>98	18	−8.1
(structure)	0.01	—	—	—
(structure)	1.9	>98	80	−85.9
(structure, Cl)	1.2	>98	71	−16.1
(structure)	0.9	>98	64	−14.5 c = 2, benzene
(structure)	0.07	>98	30	—
(structure)	0.6	>98	75	−15.0 c = 2, EtOH

Note. The following compounds were very slow substrates: cyclohexanone, methyl-4-chloro-3-oxobutanoate, 4-dimethoxy-2-butanone. The following compounds were not substrates: 2-undecanone, 2-cyclopenten-1,3-dione, 3-methyl-2-cyclohexenone, 1-phenylpropanone.

[a] Determined by gas chromatography.

[b] Determined by comparison of optical rotation values or by ^1H NMR analysis of the corresponding (+) Mosher's esters [see Ref. (7)]. All products have the (R)-configuration.

petitive inhibitor toward both 2-propanol and NAD (Figs. 9 and 10). NADH is also a noncompetitive inhibitor against 2-propanol (Fig. 11). However, NADH is a competitive inhibitor versus NAD (Fig. 12). To confirm these results, product inhibition studies were also done in the reduction of acetone by NADH. Once again, the nicotinamide cofactors were competitive inhibitors (Fig. 13). All the other inhibition patterns were noncompetitive. These patterns provide strong evidence for an ordered bi–bi mechanism as depicted in Fig. 14. A ping-pong mechanism is ruled out by the absence of uncompetitive inhibition. For a random mechanism, more than one competitive inhibition pattern at nonsaturating concentrations of substrates is expected.

Enzyme specificity. The substrate specificity of PADH is illustrated in Table 4.
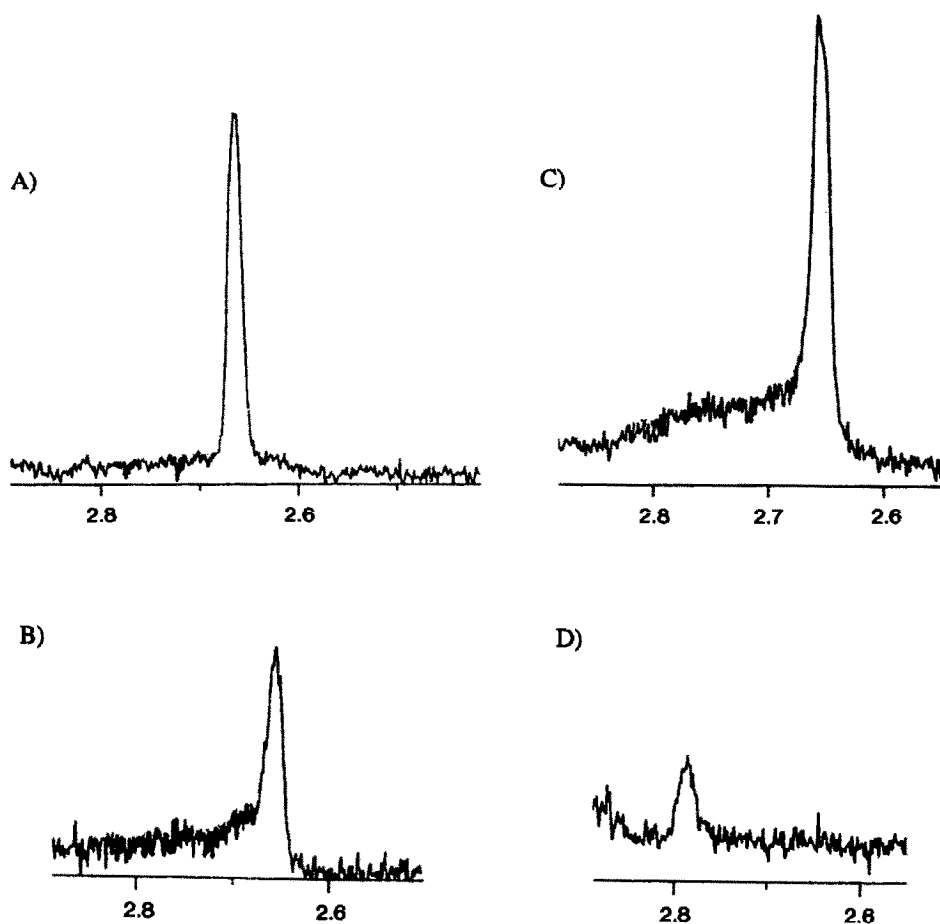
FIG. 15. Determination of stereospecificity of hydride transfer. *Pseudomonas* alcohol dehydrogenase (A) and *Thermoanaerobium brockii* alcohol dehydrogenase (B) compared to the established pro-(R) hydride transfer of yeast alcohol dehydrogenase (C) and the pro-(S) hydride transfer of glucose dehydrogenase (D). See Experimental for details.

The enzyme accepts both primary and secondary alkyl alcohols, and does not tolerate aromatic or bulky groups. PADH reduces ketones to (R)-alcohols with high enantioselectivity. The stereochemistry of the products was determined by comparison to literature values for optical rotation or by conversion to Mosher esters and determined by ^{1}H NMR. This is also reflected by the preference for (R)-alcohol oxidation over (S)-alcohols. The stereochemistry with respect to the cofactors was determined by NMR (10). The magnetic resonance peaks for pro-(R) and pro-(S) hydrogens for NADH are 2.77 and 2.67 ppm, respectively. The peak for NAD is at 8.95 ppm. Thus, by beginning with NADH deuterated only at one position, monitoring the NMR for a peak at 8.95 ppm would indicate stereochemistry. Alternatively, beginning with deuterated alcohols and NAD, the stereochemis-
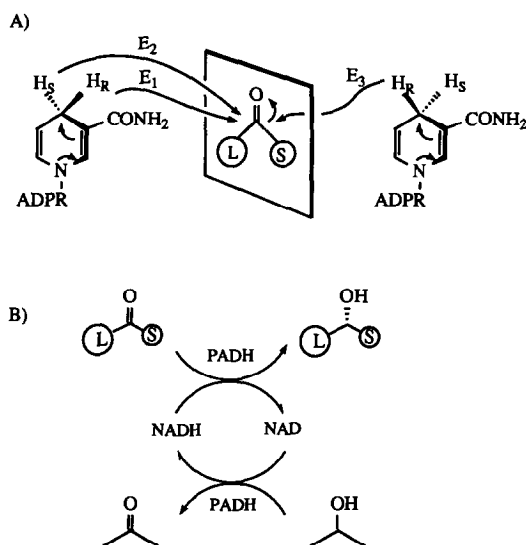
A)

B)

FIG. 16. (A) Overall stereochemical course of alcohol dehydrogenase-catalyzed reactions; E_1: *Pseudomonas* SBD6, E_2: *Mucor javanicus*, E_3: yeast, horse liver, and *Thermoanaerobium brockii*. (B) Preparative syntheses of (R)-alcohols using PADH.

try is evident by which peak at 2.67 or 2.77 ppm appears. The latter method was successfully employed for PADH. Incubation of PADH with fully deuterated 2-propanol and NAD followed by purification of deuterated NADH showed transfer of deuterium to the A face (or *re* face) of NAD by virtue of a peak at 2.67 ppm for the resulting [4A-^{2}H]NADH, indicating the enzyme is specific for the *pro-(R)* hydrogen of NADH. The results were compared with enzymes of known cofactor specificity (using appropriate deuterated substrates); horse liver alcohol dehydrogenase (A face), yeast alcohol dehydrogenase (A face), and glucose dehydrogenase (B face) (*10*). Additionally, *T. brockii* alcohol dehydrogenase has the same cofactor specificity as the other alcohol dehydrogenases, but utilizes NADP. The purified enzyme thus transfers the *pro-(R)* hydrogen from NADPH to the *re* face of the carbonyl (Fig. 15).

CONCLUSION

The NAD-dependent alcohol dehydrogenase PADH has been purified to homogeneity. The kinetic mechanism has been determined to be ordered bi–bi, with the nicotinamide cofactor being bound first followed by the substrate. The product is then released followed by the reacted cofactor. The enzyme accepts a range of small aliphatic alcohols and ketones, but does not tolerate bulky or aromatic groups. Although most alcohol dehydrogenases follow Prelog's rule in the reduction of ketones to give (*S*)-alcohols, the enzyme PADH forms exclusively (*R*)-

alcohols (*11*). It transfers the *pro*-(*R*) hydride of the nicotinamide cofactor to the *si* face of the carbonyl group. In the opposite direction, the hydride is removed from the (*R*) alcohol and transferred to the A face of NAD. This stereospecificity is unique among alcohol dehydrogenases. The overall stereochemical course of the hydride transfer catalyzed by PADH and other alcohol dehydrogenases is depicted in Fig. 16. As described previously (*3*), in the presence of 2-propanol, the enzyme is useful for the preparative synthesis of a number of secondary alcohols with very high enantiomeric excess.

ACKNOWLEDGMENT

REFERENCES

1. PRELOG, V. (1968) *Pure Appl. Chem.* **9**, 119–130.
2. (*a*) JONES, J. B. (1985) *in* Enzymes in Organic Synthesis, Ciba Foundation Symposium III, pp. 3–21, Pitman, London; (*b*) Jones, J. B. (1976) *in* Applications of Biochemical Systems in Organic Chemistry (Jones, J. B., Sih, C. J., Perlman, D., Eds.), Part 1, pp. 107–401, Wiley, New York.
3. SHEN, G. J., WANG, Y. F., BRADSHAW, C., AND WONG, C.-H. (1990) *J. Chem. Soc. Chem. Commun.*, 677–679.
4. This strain has been deposited in ATCC (ATCC 49688).
5. LAEMMLI, U. K. (1970) *Nature* **227**, 680–685.
6. HEUKESHOVEN, J., AND DERNICK, R. (1988) *Electrophoresis* **9**, 60–61.
7. KRIEG, N. R., AND HOLT, J. G. (1984) Bergey's Manual of Systematic Bacteriology, Vol. 1, pp. 140–199, Williams and Wilkins, Baltimore.
8. (*a*) CLELAND, W. W. (1963) *Biochim. Biophys. Acta* **67**, 188–196; (*b*) Cleland, W. W. (1986) *in* Techniques of Chemistry (Bernasconi, C. F., Ed.), Invest. Rates Mech. React. 4th ed. Part 1, Vol. 6, pp. 791–870, Wiley, New York.
9. SCOPES, R. K. (1982) Protein Purification Springer-Verlag, New York.
10. ARNOLD, L. J., YOU, K.-S., ALLISON, W. S., AND KAPLAN, N. O. (1976) *Biochemistry* **15**, 4844–4849.
11. Two other alcohol dehydrogenases were reported to form (*R*)-alcohols: (*a*) Hou, C. T., Patel, R., Barnabe, N., and Marczak, I. (1981) *Eur. J. Biochem.* **119**, 359–364; (*b*) Schütte, H., Hummel, W., and Kula, M.-R. (1982) *Biochim. Biophys. Acta* **716**, 298–307.